

## Supporting information

### **Electrodeposited Superaerophobic Nickel Catalyst on Pencil-Drawn Paper: A Novel Approach for Highly Efficient and Stable Hydrogen Evolution**

*Qian Sun<sup>1</sup>, Xiaoyu Hao<sup>1</sup>, Tianyi Zhang<sup>1</sup>, Zelin Ma<sup>1</sup>, Kui Hu<sup>6</sup>, Ming Yang<sup>4,5\*</sup>, Xiaolei Huang<sup>3\*</sup>, Xuqin Liu<sup>1,2\*</sup>*

<sup>1</sup> State Key Laboratory of Solidification Processing, Center of Advanced Lubrication and Seal Materials, Northwestern Polytechnical University, Xi'an, Shaanxi 710072, P. R. China.

<sup>2</sup> Shandong Laboratory of Yantai Advanced Materials and Green Manufacture, Yantai, 264006, China

<sup>3</sup> Institute of Material and Chemistry, Ganjiang Innovation Academy, Chinese Academy of Sciences, Ganzhou, 341000, China.

<sup>4</sup> Department of Applied Physics, The Hong Kong Polytechnic University, Hung Hom, Kowloon, Hong Kong SAR, China.

<sup>5</sup> Research Centre on Data Sciences & Artificial Intelligence, The Hong Kong Polytechnic University, Hung Hom, Kowloon, Hong Kong SAR, China.

<sup>6</sup> Department of Chemistry, University of Manchester, Manchester, M13 9PL, UK.

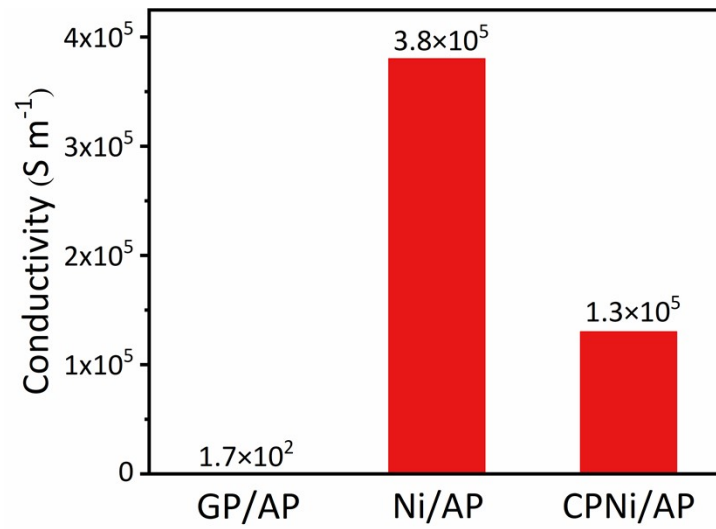


Figure S1. GP/AP, Ni/AP and CPNi/AP's conductivity chart.

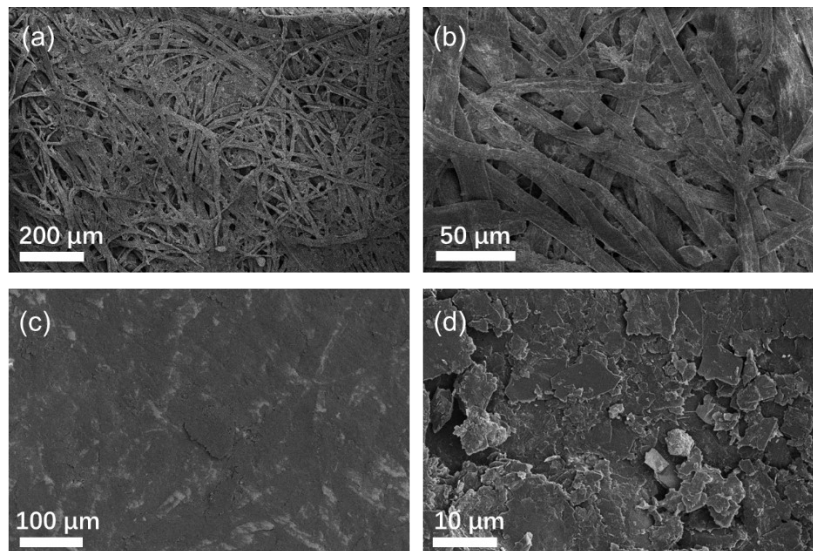


Figure S2. (a)-(b) SEM images of A4 paper and (c)-(d) GC/AP at different magnifications.

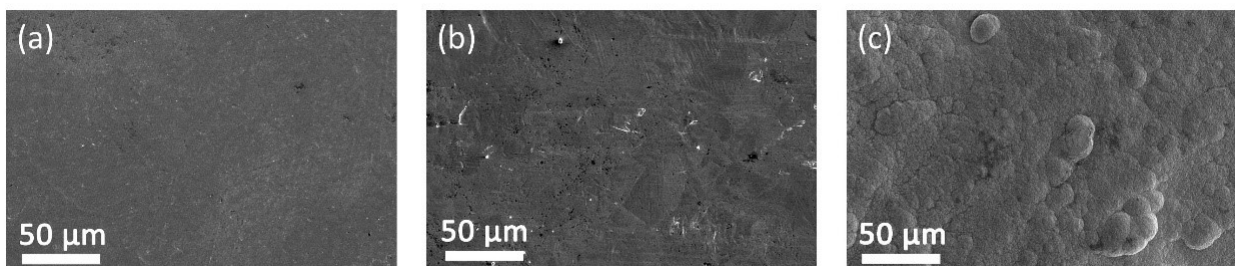


Figure S3. SEM images of (a) Pt Plate, (b) Ni Plate, and (c) Ni/AP.

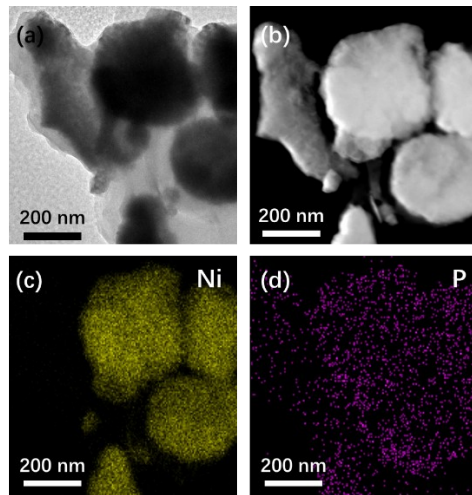


Figure S4. (a) TEM images, (b) HAADF-TEM images of CPNi/AP, and (c)-(d) corresponding Ni and P EDS images.

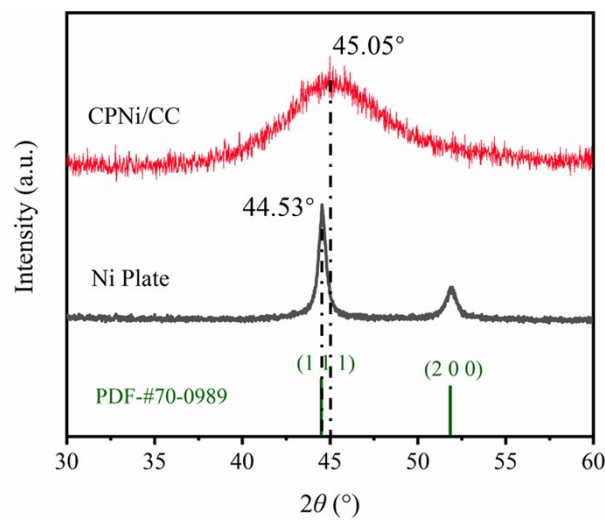


Figure S5. XRD patterns of Ni Plate, cracked phosphorus doped nickel plating on carbon cloth (CPNi/CC) at 30° to 60° magnification intervals.

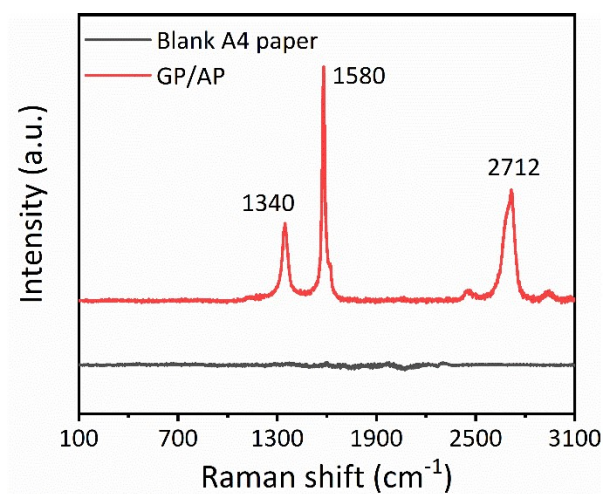


Figure S6. Raman spectra of the blank A4 paper and GP/AP.

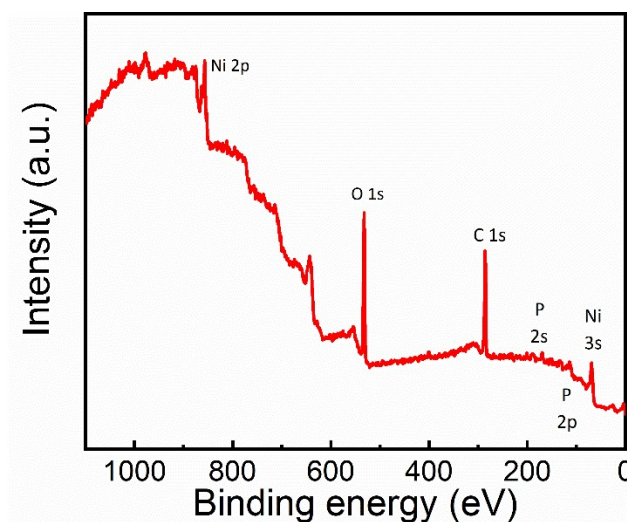


Figure S7. XPS survey spectrum of CPNi/AP.

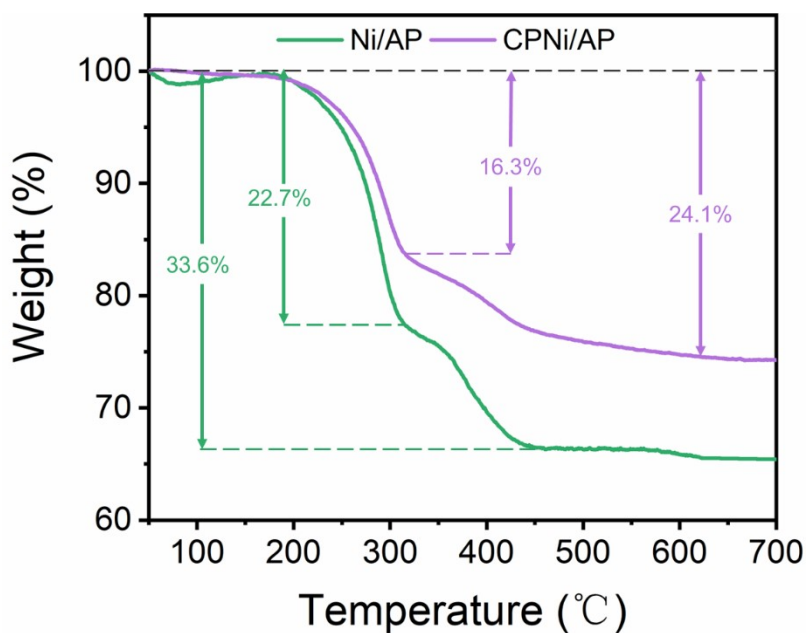


Figure S8. TG curves of CPNi/AP and Ni/AP.

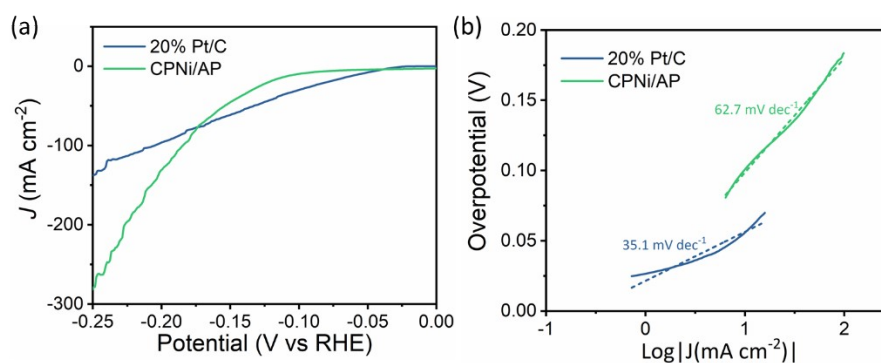


Figure S9. (a) HER polarization curves and (b) Tafel plots of 20% Pt/C and CPNi/AP in 1.0M KOH solution at a scan rate of  $1 \text{ mV s}^{-1}$ .

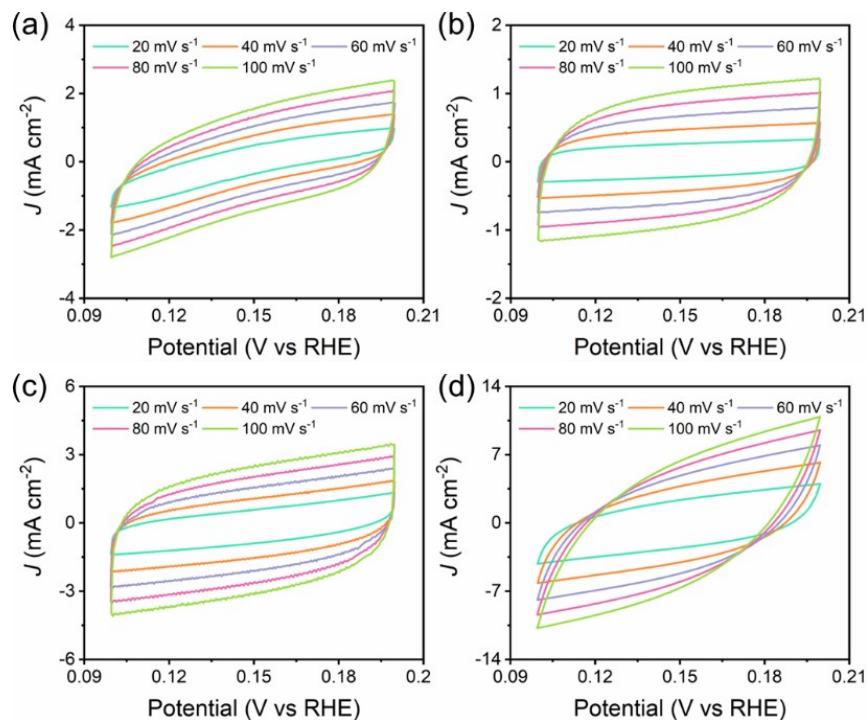


Figure S10. CV curves of (a) Pt plate, (b) Ni plate, (c) Ni/AP and (d) CPNi/AP with different current density.

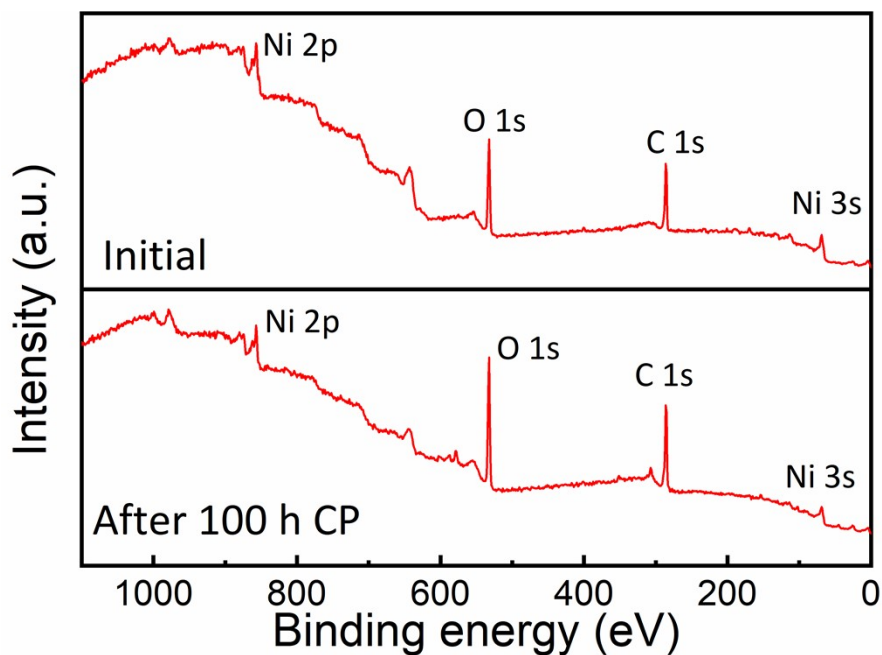


Figure S11. XPS survey spectra of CPNi/AP before and after the chronopotentiometry tests with a constant current density of 10 mA cm<sup>-2</sup> for 100 h.

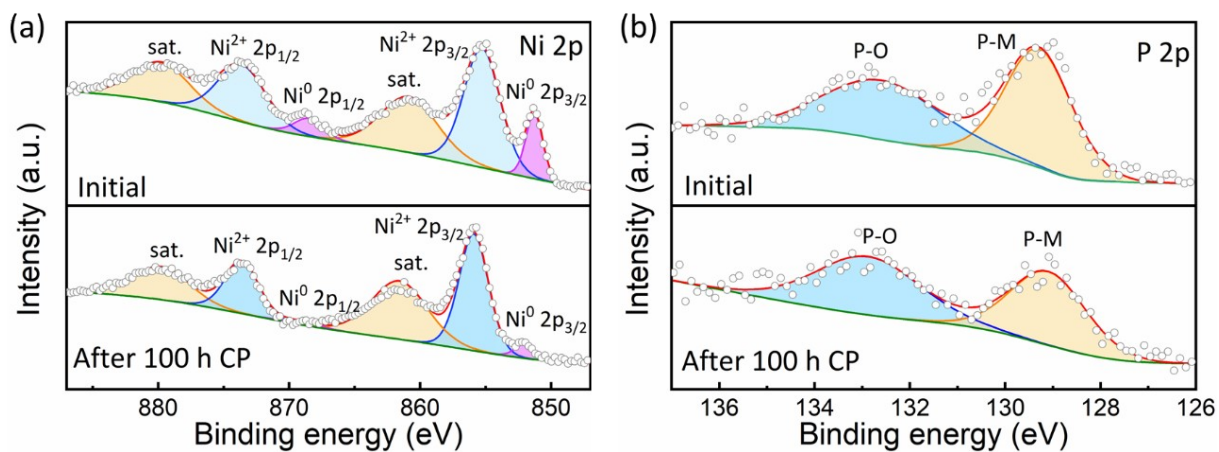


Figure S12. High-resolution XPS spectra of (a) Ni 2p and (b) P 2p in CPNi/AP before and after the chronopotentiometry tests with a constant current density of  $10 \text{ mA cm}^{-2}$  for 100 h.

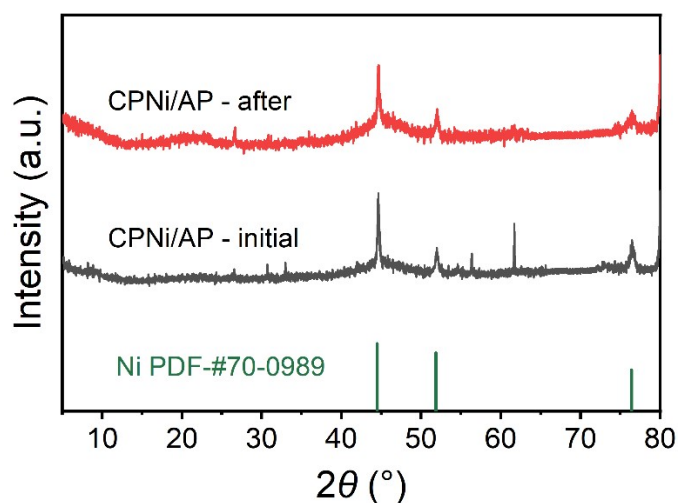


Figure S13. XRD patterns of CPNi/AP before and after reaction.

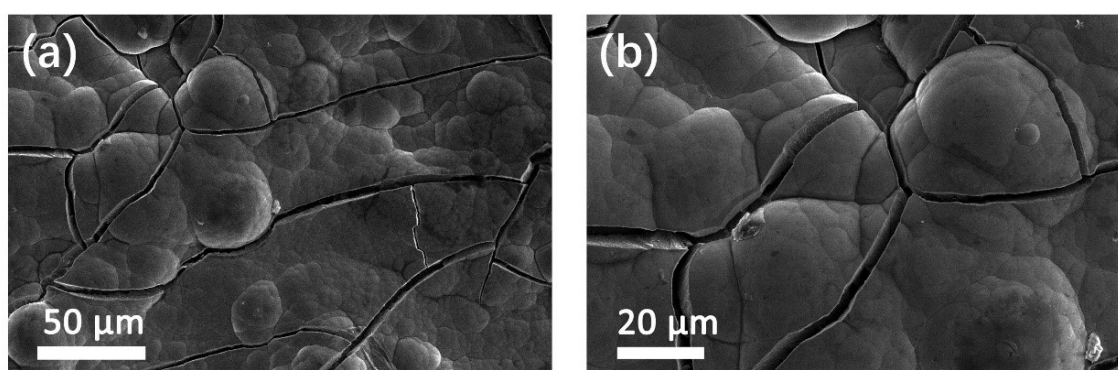


Figure S14. SEM images of CPNi/AP at different magnifications after 100 h CP test.

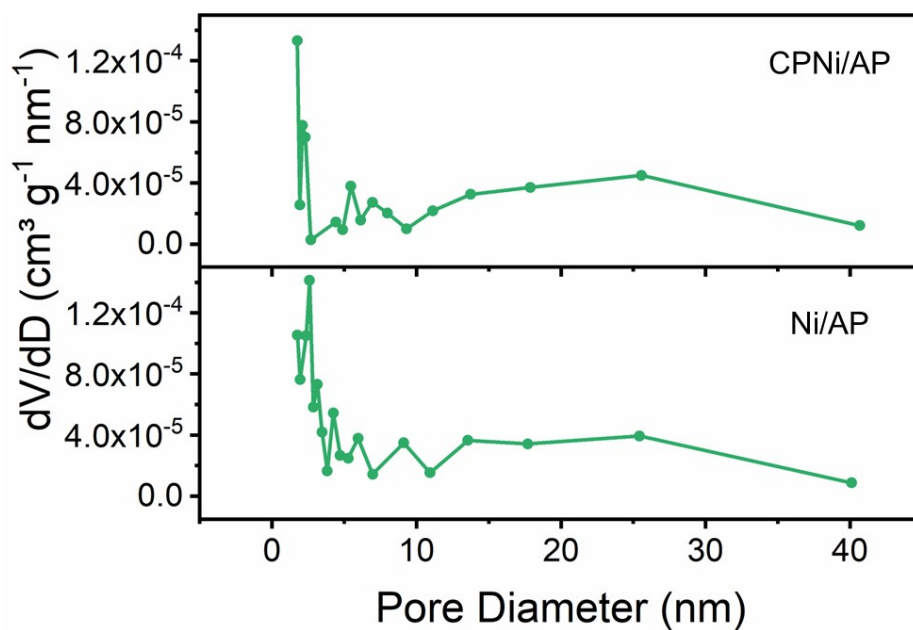


Figure S15. Pore size distribution of CPNi/AP and Ni/AP.

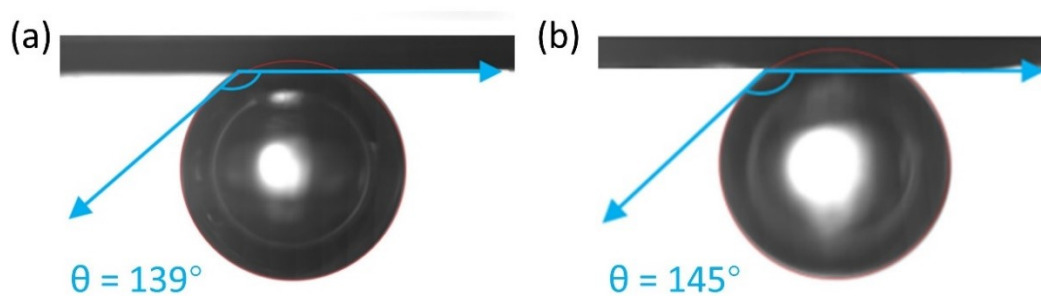


Figure S16. The gas bubble contact angles of (a) Ni plate and (b) Ni/AP.

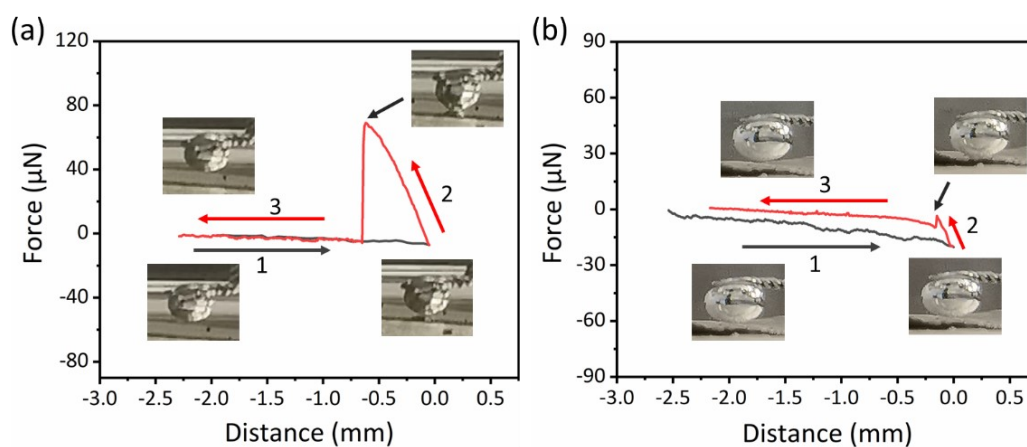


Figure S17. Adhesive forces measurements of the gas bubbles on (a) Ni plate and (b) Ni/AP.

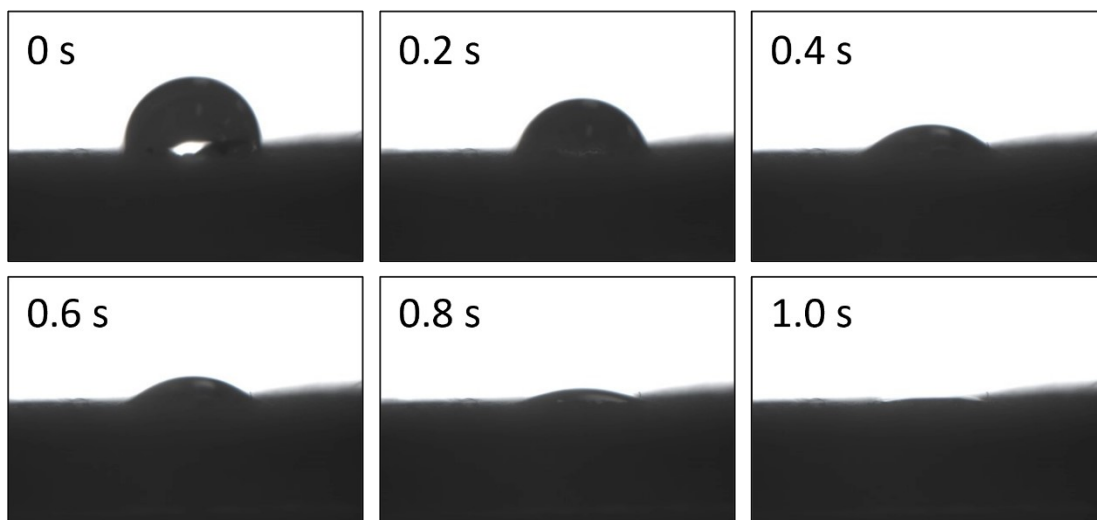


Figure S18. Contact angle of CPNi/AP.



Table S1. Selected summary of the HER performance of some Ni<sub>x</sub>P catalysts.

Catalyst	Substrate	Electrolyte	Overpotential (mV)		Synthetic method	Ref.
			$\eta_{10}$	$\eta_{100}$		
Ni <sub>2</sub> P nanosheets	Glassy carbon	1 M KOH	168		Hydrothermal	[1]
Ni <sub>5</sub> P <sub>4</sub> Nanocrystalline	Glassy carbon	1 M KOH	49	202	Solvothermal	[2]
Ni <sub>12</sub> P <sub>5</sub> hollow	Glassy carbon	1 M KOH	208		Thermal decomposition	[3]
NiP <sub>x</sub> nanospheres	Glassy carbon	0.1 M buffer solution	230	360*	Electrosynthesis	[4]
NiP <sub>2</sub> nanosheet arrays	Carbon cloth	0.5 M H <sub>2</sub> SO <sub>4</sub>	75	204	Hydrothermal	[5]
Ni <sub>5</sub> P <sub>4</sub> nanosheets	Glassy carbon	1 M KOH	147		Ice-templating	[6]
Ni <sub>2</sub> P	Carbon cloth	1 M KOH	114	290*	Hydrothermal	[7]
Ni <sub>2</sub> P	Ni foam	1 M KOH	207	400*	Hydrothermal	[8]
Fe-Ni <sub>2</sub> P	Ni foam	1 M KOH	75	226	Hydrothermal	[9]
Ni-P	Ni foam	1 M KOH	200	310	Hydrothermal	[10]
Ni <sub>2</sub> P	Porous carbon	0.5 M H <sub>2</sub> SO <sub>4</sub>	194		Thermal decomposition	[11]
Ni-P	Carbon nanotubes	1 M KOH	126		Powder sintering	[12]
NiP	Glassy carbon	1 M KOH	155	400*	Hydrothermal	[13]
HP Ni-P	RDE	1 M KOH	99	144	Electrodeposition	[14]
Ni <sub>2</sub> P/Ni <sub>12</sub> P <sub>5</sub>	Ni foam	1 M KOH	95	203	Hydrothermal	[15]
CPNi/AP	A4 paper	1 M KOH	101	183	Electrodeposition	Current work

\* Based on estimation of the LSV curves in the article.

Table S2. The  $R_{ct}$  values for different electrodes in 1 M KOH.

Electrode	Electrolyte	$R_{ct}(\Omega)$
Pt plate		7.2
Ni plate	1 M KOH	12.6
Ni/AP		5.3
CPNi/AP		2.0

Table S3. Table of volume change of  $Ni_{27-x}P_x$ .

The number of x in $Ni_{27-x}P_x$	The volume of lattice ( $\text{\AA}^3$ )					Average volume( $\text{\AA}^3$ )
	Atomic structure model 1	Atomic structure model 2	Atomic structure model 3	Atomic structure model 4	Atomic structure model 5	
0	291.33					291.33
1	290.80	290.42	290.77	290.42		290.60
2	289.54	289.54	289.54	289.54	287.89	289.21
3	288.33	288.63				288.48

## References

- [1] Q. Wang, Z. Liu, H. Zhao, H. Huang, H. Jiao and Y. Du, MOF-derived porous Ni<sub>2</sub>P nanosheets as novel bifunctional electrocatalysts for the hydrogen and oxygen evolution reactions. *J. Mater. Chem. A*, 2018, **6**, 18720-18727.
- [2] A. Laursen, K. Patraju, M. Whitaker, M. Retuerto, T. Sarkar, N. Yao, K. V. Ramanujachary, M. Greenblatt and G. C. Dismukes, Nanocrystalline Ni<sub>5</sub>P<sub>4</sub>: a hydrogen evolution electrocatalyst of exceptional efficiency in both alkaline and acidic media. *Energ. Environ. Sci.*, 2015, **8**, 1027-1034.
- [3] Y. Pan, Y. Liu, J. Zhao, K. Yang, J. Liang, D. Liu, W. Hu, D. Liu, Y. Liu and C. Liu, Monodispersed nickel phosphide nanocrystals with different phases: synthesis, characterization and electrocatalytic properties for hydrogen evolution. *J. Mater. Chem. A*, 2015, **3**, 1656-1665.
- [4] M. Chen, J. Qi, W. Zhang and R. Cao, Electrosynthesis of NiP<sub>x</sub> nanospheres for electrocatalytic hydrogen evolution from a neutral aqueous solution. *Chem. Commun*, 2017, **53**, 5507-5510.
- [5] P. Jiang, Q. Liu and X. Sun, NiP<sub>2</sub> nanosheet arrays supported on carbon cloth: an efficient 3D hydrogen evolution cathode in both acidic and alkaline solutions, *Nanoscale*, 2014, **6**, 13440-13445.
- [6] S. Lai, C. Lv, S. Chen, P. Lu, X. She, L. Wan, H. Wang, J. Sun, D. Yang, X. Zhao, Ultrathin nickel phosphide nanosheet aerogel electrocatalysts derived from Ni-alginate for hydrogen evolution reaction. *J. Alloy. and Compd*, 2020, **817**, 152727.
- [7] Y. Sun, W. Cao, X. Ge, X. Yang, Y. Wang, Y. Xu, B. Ouyang, Q. Shen and C. Li, Built-in electric field induced interfacial charge distributions of Ni<sub>2</sub>P/NiSe<sub>2</sub>

heterojunction for urea-assisted hydrogen evolution reaction, *Inorg. Chem. Front.*, 2023, **10**, 6674-6682.

[8] M. Ma, W. Xia, W. Liu, X. Guo, D. Cao and D. Cheng, Constructing NiMoP nanorod arrays with a highly active Ni<sub>2</sub>P/NiMoP<sub>2</sub> interface for hydrogen evolution in 0.5 M H<sub>2</sub>SO<sub>4</sub> and 1.0 M KOH media, *Mater. Chem. Front.*, 2023, **7**, 4029-4039.

[9] J. Zhang, J. Wang, H. Zhang, Y. Hu and H. Jiang, Chunzhong Li, Hierarchically Heterostructured Ni(OH)<sub>2</sub>/Fe–Ni<sub>2</sub>P Nanoarray: A Synergistic Electrocatalyst for Accelerating Alkaline Hydrogen Evolution, *ACS Sustainable Chem. Eng.* 2023, **11**, 458–463.

[10] Q. Xu, P. Wang, L. Wan, Z. Xu, M. Z. Sultana and B. Wang, Superhydrophilic/Superaerophobic Hierarchical NiP<sub>2</sub>@MoO<sub>2</sub>/Co(Ni)MoO<sub>4</sub> Core–Shell Array Electrocatalysts for Efficient Hydrogen Production at Large Current Densities, *ACS Appl. Mater. Interfaces* 2022, **14**, 19448–19458.

[11] Y. Lin, J. Zhang, Y. Pan and Y. Liu, Nickel phosphide nanoparticles decorated nitrogen and phosphorus co-doped porous carbon as efficient hybrid catalyst for hydrogen evolution, *Appl. Surf. Sci.*, 2017, **422**, 828–837.

[12] D. Li, W. Lan, Z. Liu and Y. Xu, Powder sintered Ni-P/CNTs composites as three-dimensional self-supported efficient electrocatalysts for hydrogen evolution reaction, *J. Alloys Compd.*, 2020, **825**, 153920.

[13] Y. Hou, Z. Yuan, X. Yu, B. Ma, L. Zhao and D. Kong, Directly preparing well-dispersed ultra-hydrophilic NiFeP nanoparticle/Mxene complexes from spent electroless Ni plating solution as efficient hydrogen evolution catalysts, *J. Environ.*

Chem. Eng., 2023, **11**, 109738.

[14] D. Song, D. Hong, Y. Kwon, H. Kim, J. Shin, H. Lee and E. Cho, Highly porous Ni-P electrode synthesized by an ultrafast electrodeposition process for efficient overall water electrolysis, *J. Mater. Chem. A*, 2020, **8**, 12069-12079.

[15] T. Zhao, S. Wang, Y. Li, C. Jia, Z. Su, D. Hao, B. Ni, Q. Zhang and C. Zhao, Heterostructured V-Doped Ni<sub>2</sub>P/Ni<sub>12</sub>P<sub>5</sub> Electrocatalysts for Hydrogen Evolution in Anion Exchange Membrane Water Electrolyzers, *Small*, 2022, **18**, 2204758.